Energy & Environmental Science

Accepted Manuscript

ROYAL SOCIETY OF CHEMISTRY

www.rsc.org/ees

Manuscript

Air-processed polymer tandem solar cells with power conversion efficiency exceeding 10%

Ning Li[1] & Christoph J. Brabec[1,2]

[1] Institute of Materials for Electronics and Energy Technology (i-MEET), Friedrich-Alexander University Erlangen-Nürnberg, Martensstraße 7, 91058 Erlangen, Germany

[2] Bavarian Center for Applied Energy Research (ZAE Bayern), Haberstraße 2a, 91058 Erlangen, Germany

*Correspondence should be addressed to Ning Li. Email: Ning.Li@fau.de; Tel.: +49 (0)9131 - 8527634; Fax: +49 (0)9131 - 8528495.

Keywords: ((Organic photovoltaics; Organic tandem solar cells; PTB7-Th, PBDTTT-EFT or PCE10; Solvent treatment; Air-processing))

The power conversion efficiencies (PCEs) of the state-of-the-art organic tandem solar cells are steadily improved in the range of 10-12%, which can be mainly attributed to the design and development of highly efficient absorbers with complementary absorption spectra. However, the impressive record efficiencies are only achieved for devices spin-coated in an inert atmosphere, which does not directly contribute to commercialization of the organic photovoltaic technology. Here, we perform a systematic study of PTB7-Th based single-junction solar cells fabricated under various conditions. The relatively low photovoltaic performance and poor environmental stability of the air-processed devices are successfully recovered by a post-treatment with alcohol-based solvents. The effect of solvent treatment is valid for both regular and inverted device architecture. Tandem devices fabricated by doctor-blading in air achieve a high PCE of 10.03% along with an unprecedented high FF of 76.6%.

Introduction

Organic photovoltaics (OPV) has attracted tremendous research attentions in the last decade, owing to its novel properties, practical applicability and low-cost large-scale manufacturing.[1-12] The power conversion efficiencies (PCEs) of single-junction OPV devices have been continuously improved to ~11%,[13] and are supposed to approach the 15% theoretical limit by designing and developing novel absorbing materials with reduced bandgap-voltage offset along with high fill factor (FF) and external quantum efficiency (EQE).[3] Compared to their inorganic counterparts, the relatively narrow absorption windows of the organic absorbers inevitably restrict the utilization of photons, thus limiting their performances.

The tandem architecture, in which two or more sub-cells with complementary absorption spectra are monolithically stacked together and connected in series, has been proven as one of the most promising concepts to address the losses related to the narrow absorption of organic absorbers.[14-17] The loss due to thermalization of the excess energy photons can also be simultaneously minimized by combining the absorbers possessing different bandgaps in a tandem architecture. The high-energy photons can be absorbed in the front-placed wide bandgap donor to deliver high open circuit voltage (V_{OC}), while the photons with energy lower than the bandgap of the front donor can be absorbed by the back-placed low bandgap donor and enhance a more complete utilization of photons. It has been calculated that double-junction tandem OPV devices have the theoretical potential to exceed the 20% efficiency benchmark.[18]

The PCEs of the state-of-the-art tandem OPV devices have been steadily improved in the range of 10-12% over the last few years, which can be mainly attributed to the design and development of highly efficient absorbers with complemental absorption spectra.[19-25] Moreover, the currently emerged novel absorbers, such as low-bandgap donors with absorption onsets over 900 nm exhibiting unprecedented photocurrents,[26-28] absorbers with moderate bandgaps[29-31] exhibiting extremely high FF and EQE as well as absorbers with large bandgaps[32-34] showing high V_{OC} along with promising short circuit current (J_{SC}), have already achieved promising photovoltaic performance for single-junction as well as tandem OPV devices. By fine-tuning the bandgap and thickness of an organic absorber for a respective sub-cell in combination with the advanced process technology, these novel absorbers have the great potential to continuously close the efficiency gap between the experimental achievements and the theoretical limitations.

Poly[4,8-bis(5-(2-ethylhexyl)thiophen-2-yl)benzo[1,2-b;4,5-b']dithiophene-2,6-diyl-alt-(4-(2-ethylhexyl)-3-fluorothieno[3,4-b]thiophene-)-2-carboxylate-2-6-diyl)], commonly known as PCE10, PBDTTT-EFT or PTB7-Th, has been reported for highly-efficient single-junction OPV devices with PCEs >10%.[29, 30, 35-37] The bandgap of ~1.6 eV makes this absorber very attractive for the tandem concept, and the tandem solar cells based on two identical PTB7-Th sub-cells have reached PCEs as high as 11.3%.[20] According to the calculation, an absorber with a bandgap of ~1.2 eV would be an ideal counterpart for PTB7-Th in the tandem architecture to achieve ultra-high performance.[18] Moreover, a promising alternative would be to combine an extra-wide bandgap absorber and an extra-low bandgap absorber with the PTB7-Th for a triple-junction architecture, which has been successfully demonstrated to acquire superior performance compared to the single- as well as the double-junction reference devices.[22-24]

However, similar as other BDT-based polymers, the PTB7-Th shows poor environmental stability, and is easily oxidized in the presence of oxygen and light, which is a serious obstacle to large-scale production under ambient conditions.[38] Therefore, the very impressive performances reported until now were exclusively achieved by spin-coating the active layer in inert atmosphere which is absolutely incompatible with roll-to-roll manufacturing. Several studies have been performed by means of transient absorption spectroscopy,[39] Fourier transform infrared spectroscopy[40] and Raman spectroscopy[41] to understand the oxidation mechanisms of the BDT-based polymers. These studies proposed several approaches to describe the degradation and oxidation mechanisms of the BDT-based polymers and gave valuable inside into design and development of more stable polymers for the future. However, no study has been reported on the successful fabrication of efficient BDT-based polymers, such as PTB7-Th, under ambient conditions using roll-to-roll or compatible production methods.

In this work, we perform a systematic comparison of the PTB7-Th based single-junction solar cells fabricated under various conditions. The fabrication of the PTB7-Th based devices is stepwise transferred from spin-coating to doctor-blading and from an inert atmosphere to air conditions. The relatively low photovoltaic performances of the air-processed devices are successfully recovered by the treatment with alcohol-based solvents. The PTB7-Th solar cells fabricated in air using doctor-blading achieve superior photovoltaic performance and environmental stability to the references that are spin-coated in a nitrogen-filled glove box. Furthermore, we construct tandem solar cells by combining PTB7-Th based sub-cells with a commercially available polymer. Tandem devices fabricated by doctor-blading in air achieve a fully additive V_{OC} of 1.55V, a J_{SC} of 8.45 mA cm^{-2} and an unprecedented FF of 76.6%, resulting in a high PCE of 10.03%.

Results and Discussion

Fig. 1a illustrates the deposition methods used in this work to fabricate the PTB7-Th based solar cells. The solar cells in regular architecture were fabricated under 3 different conditions: 1) spin-coated in a nitrogen-filled glove box; 2) spin-coated in air and 3) doctor-bladed in air. PTB7-Th:PC$_{70}$BM (1:1.5 wt.%) were dissolved in chlorobenzene with 3% 1,8-diiodooctane (DIO), and the active layer thickness was optimized to ~120 nm. Solar cells spin-coated in nitrogen atmosphere served as reference devices and exhibited an average PCE of ~8%. The devices processed in air by either spin-coating or doctor-blading suffered from relatively low FF and J_{SC}, although the active layers deposited under different conditions exhibited very similar absorption spectra, as shown in Fig. 1b. Owing to its low volatility, a small amount of DIO always remained in the active layer after drying and obviously results in undried and easily removable thin films. Although DIO is expected to be removed from the active layer under high vacuum (10^{-6} mbar) during thermal-evaporation of the top electrode, we find that a small amount of this additive remains in the active layer and indeed has a negative effect on the device performance when exposed to air.

The air-processed active layers were then treated under different conditions to remove the residual DIO, as depicted in Supplementary Fig. S1 and S2. The residual DIO in the pristine polymer and blends can be removed by 1) thermal-annealing at 140°C for 10 min; 2) drying in air for 24h; 3) drying in vacuum (0.1 mbar) for 24h and 4) spin-coating or doctor-blading methanol on top of the active layer. However, only the methanol treatment could recover the performance of the air-processed PTB7-Th solar cells. As summarized in Figure 1c and Table 1, the photovoltaic performances of the air-processed devices, especially in J_{SC} and FF, were significantly improved by methanol treatment. The devices doctor-bladed in air achieved an average PCE of 8.31%, showing equal or even superior performance to the reference devices. For comparison, the photovoltaic performances of the air-processed devices treated under different conditions are summarized in Supplementary Fig. S3 and Table S1.

Fig. S4 and S5 illustrate the optical microscopy and atomic force microscopy (AFM) images of thins films prepared under different conditions. PTB7-Th and PTB7-Th:$PC_{70}BM$ thin films with 3% DIO were deposited on glass substrates in air and either dried in vacuum or otherwise treated with methanol. Neither the microscope nor the AFM images reveal a significant difference between these two processing methods, although the PTB7-Th:$PC_{70}BM$ samples treated with methanol do show a slightly reduced contact angle for water. Moreover, it can be seen from the AFM images, that all the samples show fairly smooth surfaces with a root-mean-square (Rms) roughness of ~1 nm. To demonstrate the general validity and importance of the washing process for BDT-based polymers, we decided to further extend these tests towards another relevant representative of the BDT-polymer class, namely poly[[4,8-bis[(2-ethylhexyl)oxy]benzo[1,2-b:4,5-b']dithiophene-2,6-diyl][3-fluoro-2-[(2-ethylhexyl)carbonyl]thieno[3,4-b]thiophenediyl]] (PTB7). Again, we observe a significant impact on performance due to the solvent washing. The J-V characteristics of PTB7 single junction cells fabricated under different conditions are summarized in Fig. S6 and Table S2. The efficiency, J_{SC} and FF of environmentally bladed PTB7 single cells are significantly improved by the methanol treatment, from app 3 % to over 6 %. Washing with methanol actually resulted in a performance comparable to the optimized devices fabricated by spin-coating in inert conditions.

It has been reported that the BDT-based devices degrade very quickly in the presence of oxygen and light.[41] We found that PTB7-Th showed poor environmental stability in the presence of DIO and that the stability became even worse when PTB7-Th is embedded between electrodes as typical for real device architectures, i.e. mixed with PCBM and coated on top of the interfacial layer, such as poly(3,4-ethylenedioxythiophene)-poly(styrenesulfonate) (PEDOT:PSS) or polyethylenimine (PEI). As shown in Supplementary Fig. S4, the color of the PTB7-Th:$PC_{70}BM$ thin film clearly changed within 30 min after deposition by doctor-blading in air on top of the PEDOT:PSS. The residual additive DIO could on the one hand behave as chromophoric impurities which absorb UV light and produce radicals which react further with the polymer,[42,43] and on the other hand form effective percolation pathways for oxygen while remaining in the active layer. The residual additive DIO is expected to be removed from the active layer by treating with alcoholic solvent, such as methanol,[44-46] resulting in a dense and well-packed active layer. The samples treated with methanol showed very promising environmental stability, which is verified by the absorption spectra measured under continuous light illumination, as depicted in Fig. 2a.

However, from a production point of view, the highly toxic and volatile methanol is undesired and disadvantageous for large-scale production. Under the same processing conditions, various commonly used solvents, such as acetone, ethanol and isopropyl alcohol, were tested by doctor-blading thin layers of solvent on top of the active layer in air. The *J-V* characteristics of the corresponding devices are summarized in Fig. 2b and Table 2. The performance of the air-processed devices can be recovered by the solvent treatment with alcohol-based solvents, while the treatment with a non-alcoholic solvent, such as acetone, does not show the same advantageous effect. According to our experimental results, the devices treated with ethanol achieved slightly higher performance compared to the methanol treated references, although the treatment with methanol was reported to achieve the best performance for the BDT-based polymers.[47] From a technical standpoint, the treatment with ethanol would provide more space for large-scale production under various conditions, such as processing at elevated temperatures.

The treatment with alcohol-based solvent also works well for devices in the inverted architecture (ITO/PEI/PTB7-Th:PC70BM/MoOx/Ag). As shown in Fig. 2c, the devices treated with ethanol exhibited a V_{OC} of 0.78 V, a J_{SC} of 16.99 mA cm^{-2} and a FF of 62.6%, resulting in a PCE of 8.30%, while the reference devices without solvent treatment again suffer from low J_{SC} and FF, resulting in an average PCE of only 4.03%. Based on the experimental results, it can be concluded that the treatment with alcoholic solvents is a bulk-effect rather than a surface modification effect. The series resistance of devices treated with alcoholic solvents is significantly reduced as compared to the control devices, indicating a better distribution of the nanostructured $PC_{70}BM$ in the polymer matrices to form bicontinuous interpenetrating networks. To demonstrate the enhanced environmental stability of the devices treated with alcoholic solvents, PTB7-Th:$PC_{70}BM$ solar cells in an inverted architecture were constructed in air with and without ethanol treatment and stored under ambient conditions without encapsulation. Device performance as a function of time is summarized in Fig. 2d. A performance reduction by >20% was observed for the control devices without solvent treatment within the first day, while the performance of devices treated with ethanol decreased only by ~2%. The control devices retained only ~45% of the initial performance after 17 days, while the devices treated with ethanol still exhibited ~76% of the initial performance after 30 days.

Tandem solar cells in the device architecture illustrated in Fig. 3a were constructed by doctor-blading in air to demonstrate the general applicability of the treatment with alcoholic solvents. Owing to its promising environmental processing properties, the GEN-2 polymer[18, 48] which is commercially available from Merck was employed in combination with PCBM for the front cell. The *J*-*V* characteristics of the GEN-2:PCBM in an inverted device architecture are depicted in Fig. 3b and Table 3. GEN-2:PCBM does achieve PCEs of >7%, which is mainly ascribed to the high FFs of >70% for devices with an active layer thickness ranging between 220 and 360 nm. The PTB7-Th:$PC_{70}BM$ back cell treated with ethanol was stacked on top of the front cell to harvest the unabsorbed photons. The efficient intermediate layer consists of PEDOT HIL3.3 and ZnO as reported in our previous publications.[18, 49] A thin layer of PEI was inserted between ZnO and PTB7-Th:$PC_{70}BM$ to reduce the charge recombination at the surface, improving the FF of the back cell up to 70%. The optimized tandem solar cell incorporating the 300 nm thick front cell and 120 nm thick back cell achieved a high PCE of 10.03% along with an unprecedented high FF of 76.6%, which to the best of knowledge was not reported before for tandem OPV devices fabricated with roll-to-roll compatible deposition methods under ambient conditions. The *J-V* characteristics of the tandem as well as corresponding single-junction solar cells are summarized in Fig. 3c and Table 3. The EQE spectra of the tandem cell under blue and IR light bias are depicted in Fig. 3d. Owing to the high EQE value of the PTB7-Th in the absorption range of 700-800 nm, the photocurrent generated in the front cell can be balanced by a thin back cell.

he unprecedented high FF obtained for the tandem solar cells, which is even higher than the assumption of 75% used for our previous theoretical efficiency predictions,[3, 18] and is mainly attributed to the high FF of the sub-cells and the fully functional intermediate layer. Compared to the J_{SC} of 10-11 mA cm^{-2} delivered by the state-of-the-art tandem OPV devices,[20, 22] the J_{SC} of 8.45 mA cm^{-2} achieved in this work is not very impressive, which can be attributed to the too strong overlapping absorption of the front and back cell. Nevertheless, the performance of the tandem OPV devices can be further improved by designing and developing novel absorbers with both promising photovoltaic parameters and air-pcoessability to approach the 21% theoretical efficiency limit. The promising photovoltaic parameters demonstrated in this work along with the facile fabrication conditions, which are fully compatible with roll-to-roll large-scale production, will attract more research interest and effort in commercialization of highly efficient tandem OPV devices.

In conclusion, we demonstrated the fabrication of highly efficient PTB7-Th based single-junction as well as tandem solar cells by doctor-blading under ambient conditions. The performance of the air-processed PTB7-Th solar cells can be recovered by a post-treatment with alcohol-based solvents. The effect of solvent treatment was not limited to a certain device architecture and worked nicely for both regular and inverted device configurations. The control devices fabricated by doctor-blading in air suffered a lot from a low J_{SC} and FF and exhibited PCEs of only ~4%, while devices treated with ethanol achieved PCEs of ~8.3% along with great shelf lifetime. Air-processed tandem solar cells incorporating GEN-2:PCBM as front and PTB7-Th:PC$_{70}$BM as back cell exhibited a high PCE of 10.03% along with a V_{OC} of 1.55V, a J_{SC} of 8.45 mA cm^{-2} and an unprecedented high FF of 76.6%.

Experimental

Materials: PTB7-Th (batch: YY8070) and GEN-2 were received from 1-Materials and Merck, respectively. PEDOT:PSS (AI 4083) and PEDOT HIL3.3 were provided by Heraeus. PCBM (99.5%) and PC$_{70}$BM (99%) were purchased from Solenne BV. ZnO-nanoparticles were received from the Technical University of Denmark (DTU) and dissolved in acetone.[50] Branched PEI solution (50 wt.% in H_2O) was purchased from Sigma-Aldrich. All the materials were used as received without further purification.

Fabrication of single-junction devices: the single-junction devices in either regular architecture (ITO/PEDOT:PSS/PTB7-Th:PC$_{70}$BM/Ca/Ag) or inverted architecture (ITO/PEI/PTB7-Th:PC$_{70}$BM/MoOx/Ag) were fabricated on ITO-coated glasses using spin-coating or doctor-blading in nitrogen atmosphere or in air. The substrate was cleaned by ultra-sonication in acetone and isopropanol for 10 minutes each, and blow-dried using a nitrogen gun. The substrate was coated with 40 nm PEDOT:PSS (regular architecture) or ~10 nm PEI (inverted architecture) and dried at 80 °C for 5 min. The active layer with a thickness of 120 nm was deposited by spin-coating in nitrogen atmosphere, or spin-coating in air or doctor-blading in air from a chlorobenzene solution of PTB7-Th:PC$_{70}$BM with a mixture ratio of 1:1.5 wt.% (20 mg/mL in total). 3 vol.% DIO was added to the solution 1 hour prior to deposition. Afterwards, the solvent treatment was performed immediately by spin-coating or doctor-blading the alcoholic solvent on top of the active layer. The solar cells were completed by thermal evaporation of 15 nm Ca/ 100 nm Ag (regular architecture) or 15 nm MoOx/ 100 nm Ag (inverted architecture) at 10^{-6} mbar.

Fabrication of tandem devices: the tandem devices were fabricated on ITO-coated glasses using doctor blading under ambient conditions. The substrate was cleaned by ultra-sonication in acetone and isopropanol for 10 minutes each. After drying, the substrate was coated with approximately 30 nm ZnO and dried at 80 °C for 5 min. The first active layer with a thickness of 300 nm was bladed from a dichlorobenzene (DCB)-based solution of GEN-2:PCBM with a mixture ratio of 1:1.5 wt.% (30 mg/mL in total). After that, ~40 nm thick PEDOT:PSS HIL3.3 (1:5, diluted in IPA) was bladed on top of the first active layer and followed by deposition of ~30 nm thick ZnO layer. Both PEDOT:PSS and ZnO layers were dried at 80 °C for 5 min in air. The ZnO layer was modified by coating 10 nm thick PEI on top, which was diluted with 2-methoxyethanol at a concentration of 1 mg/mL. The second active layer, PTB7-Th:PC$_{70}$BM, with a thickness of 120 nm was deposited and followed by solvent treatment with ethanol. Then, the whole stack was completed by thermal-evaporation of a 15 nm thick MoOx and a 100 nm thick Ag at 10^{-6} mbar.

Characterizations: All the J-V characteristics were recorded using a source measurement unit from BoTest. Illumination was provided by a solar simulator (Oriel Sol 1A, from Newport) with AM1.5G spectra at 100 mW cm^{-2}, which was calibrated by a certified silicon solar cell. The active area of the constructed OSCs were defined by the overlap of the bottom and top electrode, which was determined to be 10.4 mm^2 for the OSCs based on ITO-coated glass and vacuum-deposited top electrode. The optical and morphological properties of the electrodes were investigated by a UV-Vis-NIR spectrometer (Lambda 950, from Perkin Elmer). The extra illumination applied to the samples was supplied by a tungsten lamp, and its intensity was calibrated by a certified silicon solar cell from Newport. The thicknesses of the films were measured with a profilometer (Tencor Alpha Step D 100). The EQE spectra were recorded by an Enli Technology (Taiwan) EQE measurement system (QE-R), and the light intensity at each wavelength was calibrated with a standard single-crystal Si photovoltaic cell.

Acknowledgement

This work was financially supported by the Joint Projects Helmholtz Institute Erlangen Nürnberg (HI-ERN) under project number DBF01253 and the Cluster of Excellence "Engineering of Advanced Materials" (EAM) at Friedrich-Alexander University Erlangen-Nürnberg. We thank Heraeus, Dr. Stephane Berny from Merck, Dr. Steven Xiao from 1-Materials and Prof. Frederik C. Krebs for providing PEDOT HIL3.3, GEN-2, PTB7-Th and ZnO nanoparticles, respectively. C.J.B. gratefully acknowledges the financial support through the "Aufbruch Bayern" initiative of the state of Bavaria (EnCN and solar factory of the future) as well as the Bavarian Initiative "Solar Technologies go Hybrid" (SolTech).

References

1. A. J. Heeger, *Advanced Materials*, 2014, **26**, 10-28.
2. Z. He, H. Wu and Y. Cao, *Advanced Materials*, 2014, **26**, 1006-1024.
3. M. Scharber and N. Sariciftci, *Progress in Polymer Science*, 2013, **38**, 1929-1940.
4. L. Dou, J. You, Z. Hong, Z. Xu, G. Li, R. A. Street and Y. Yang, *Advanced Materials*, 2013, **25**, 6642-6671.
5. H.-L. Yip and A. K. Y. Jen, *Energ Environ Sci*, 2012, **5**, 5994-6011.

6. R. Søndergaard, M. Hösel, D. Angmo, T. T. Larsen-Olsen and F. C. Krebs, *Materials Today*, 2012, **15**, 36-49.
7. Y. Li, *Accounts Chem Res*, 2012, **45**, 723-733.
8. J. Nelson, *Materials Today*, 2011, **14**, 462-470.
9. C. J. Brabec, S. Gowrisanker, J. J. M. Halls, D. Laird, S. Jia and S. P. Williams, *Advanced Materials*, 2010, **22**, 3839-3856.
10. F. Machui, M. Hosel, N. Li, G. D. Spyropoulos, T. Ameri, R. R. Sondergaard, M. Jorgensen, A. Scheel, D. Gaiser, K. Kreul, D. Lenssen, M. Legros, N. Lemaitre, M. Vilkman, M. Valimaki, S. Nordman, C. J. Brabec and F. C. Krebs, *Energ Environ Sci*, 2014, **7**, 2792-2802.
11. W. Chen, M. P. Nikiforov and S. B. Darling, *Energ Environ Sci*, 2012, **5**, 8045-8074.
12. R. A. J. Janssen and J. Nelson, *Advanced Materials*, 2013, **25**, 1847-1858.
13. M. A. Green, K. Emery, Y. Hishikawa, W. Warta and E. D. Dunlop, *Progress in Photovoltaics: Research and Applications*, 2015, **23**, 1-9.
14. T. Ameri, N. Li and C. J. Brabec, *Energ Environ Sci*, 2013, **6**, 2390-2413.
15. O. Adebanjo, P. P. Maharjan, P. Adhikary, M. Wang, S. Yang and Q. Qiao, *Energ Environ Sci*, 2013, **6**, 3150-3170.
16. O. Adebanjo, B. Vaagensmith and Q. Qiao, *Journal of Materials Chemistry A*, 2014, **2**, 10331-10349.
17. J. You, L. Dou, Z. Hong, G. Li and Y. Yang, *Progress in Polymer Science*, 2013, **38**, 1909-1928.
18. N. Li, D. Baran, G. D. Spyropoulos, H. Zhang, S. Berny, M. Turbiez, T. Ameri, F. C. Krebs and C. J. Brabec, *Advanced Energy Materials*, 2014, **4**, 1400084.
19. L. Zuo, C.-Y. Chang, C.-C. Chueh, S. Zhang, H. Li, A. K. Y. Jen and H. Chen, *Energ Environ Sci*, 2015.
20. H. Zhou, Y. Zhang, C.-K. Mai, S. D. Collins, G. C. Bazan, T.-Q. Nguyen and A. J. Heeger, *Advanced Materials*, 2015, **27**, 1767-1773.
21. Z. Zheng, S. Zhang, M. Zhang, K. Zhao, L. Ye, Y. Chen, B. Yang and J. Hou, *Advanced Materials*, 2015, **27**, 1189-1194.
22. A. R. b. Mohd Yusoff, D. Kim, H. P. Kim, F. K. Shneider, W. J. da Silva and J. Jang, *Energ Environ Sci*, 2015, **8**, 303-316.
23. C.-C. Chen, W.-H. Chang, K. Yoshimura, K. Ohya, J. You, J. Gao, Z. Hong and Y. Yang, *Advanced Materials*, 2014, **26**, 5670-5677.
24. X. Che, X. Xiao, J. D. Zimmerman, D. Fan and S. R. Forrest, *Advanced Energy Materials*, 2014, **4**, 1400568.
25. J. You, L. Dou, K. Yoshimura, T. Kato, K. Ohya, T. Moriarty, K. Emery, C.-C. Chen, J. Gao, G. Li and Y. Yang, *Nature Communications*, 2013, **4**, 1446.
26. H. Choi, S.-J. Ko, T. Kim, P.-O. Morin, B. Walker, B. H. Lee, M. Leclerc, J. Y. Kim and A. J. Heeger, *Advanced Materials*, 2015, DOI: 10.1002/adma.201501132.
27. K. H. Hendriks, W. Li, M. M. Wienk and R. A. J. Janssen, *Journal of the American Chemical Society*, 2014, **136**, 12130-12136.
28. R. S. Ashraf, I. Meager, M. Nikolka, M. Kirkus, M. Planells, B. C. Schroeder, S. Holliday, M. Hurhangee, C. B. Nielsen, H. Sirringhaus and I. McCulloch, *Journal of the American Chemical Society*, 2015, **137**, 1314-1321.
29. C. Liu, C. Yi, K. Wang, Y. Yang, R. Bhatta, M. Tsige, S. Xiao and X. Gong, *ACS Applied Materials & Interfaces*, 2015, **7**, 4928-4935.
30. Z. He, B. Xiao, F. Liu, H. Wu, Y. Yang, S. Xiao, C. Wang, T. P. Russell and Y. Cao, *Nat Photon*, 2015, **9**, 174-179.
31. Y. Liu, J. Zhao, Z. Li, C. Mu, W. Ma, H. Hu, K. Jiang, H. Lin, H. Ade and H. Yan, *Nat Commun*, 2014, **5**, 5293.

32. L. Huo, T. Liu, X. Sun, Y. Cai, A. J. Heeger and Y. Sun, *Advanced Materials*, 2015, **27**, 2938-2944.
33. X. Zhu, J. Fang, K. Lu, J. Zhang, L. Zhu, Y. Zhao, Z. Shuai and Z. Wei, *Chemistry of Materials*, 2014, **26**, 6947-6954.
34. M. Zhang, X. Guo, W. Ma, H. Ade and J. Hou, *Advanced Materials*, 2014, **26**, 5880-5885.
35. L. K. Jagadamma, M. Al-Senani, A. El-Labban, I. Gereige, G. O. Ngongang Ndjawa, J. C. D. Faria, T. Kim, K. Zhao, F. Cruciani, D. H. Anjum, M. A. McLachlan, P. M. Beaujuge and A. Amassian, *Advanced Energy Materials*, 2015, **5**, 1570065.
36. J.-D. Chen, C. Cui, Y.-Q. Li, L. Zhou, Q.-D. Ou, C. Li, Y. Li and J.-X. Tang, *Advanced Materials*, 2015, **27**, 1035-1041.
37. S.-H. Liao, H.-J. Jhuo, P.-N. Yeh, Y.-S. Cheng, Y.-L. Li, Y.-H. Lee, S. Sharma and S.-A. Chen, *Sci. Rep.*, 2014, **4**, 6813.
38. L. Lu and L. Yu, *Advanced Materials*, 2014, **26**, 4413-4430.
39. Y. W. Soon, H. Cho, J. Low, H. Bronstein, I. McCulloch and J. R. Durrant, *Chem Commun*, 2013, **49**, 1291-1293.
40. H. J. Son, W. Wang, T. Xu, Y. Liang, Y. Wu, G. Li and L. Yu, *Journal of the American Chemical Society*, 2011, **133**, 1885-1894.
41. J. Razzell-Hollis, J. Wade, W. C. Tsoi, Y. Soon, J. Durrant and J.-S. Kim, *Journal of Materials Chemistry A*, 2014, **2**, 20189-20195.
42. S. Morlat and J.-L. Gardette, *Polymer*, 2001, **42**, 6071-6079.
43. J. F. Rabek and J. F. Rabek, *Photodegradation of polymers*, Springer Berlin, 1996.
44. H. Zhou, Y. Zhang, J. Seifter, S. D. Collins, C. Luo, G. C. Bazan, T.-Q. Nguyen and A. J. Heeger, *Advanced Materials*, 2013, **25**, 1646-1652.
45. L. Ye, Y. Jing, X. Guo, H. Sun, S. Zhang, M. Zhang, L. Huo and J. Hou, *The Journal of Physical Chemistry C*, 2013, **117**, 14920-14928.
46. Z. Xiao, Y. Yuan, B. Yang, J. VanDerslice, J. Chen, O. Dyck, G. Duscher and J. Huang, *Advanced Materials*, 2014, **26**, 3068-3075.
47. S. Guo, B. Cao, W. Wang, J.-F. Moulin and P. Müller-Buschbaum, *ACS Applied Materials & Interfaces*, 2015, **7**, 4641-4649.
48. N. Li, D. Baran, K. Forberich, F. Machui, T. Ameri, M. Turbiez, M. Carrasco-Orozco, M. Drees, A. Facchetti, F. C. Krebs and C. J. Brabec, *Energ Environ Sci*, 2013, **6**, 3407-3413.
49. N. Li, P. Kubis, K. Forberich, T. Ameri, F. C. Krebs and C. J. Brabec, *Sol Energ Mat Sol C*, 2014, **120**, 701-708.
50. F. C. Krebs, *Organic Electronics*, 2009, **10**, 761-768.

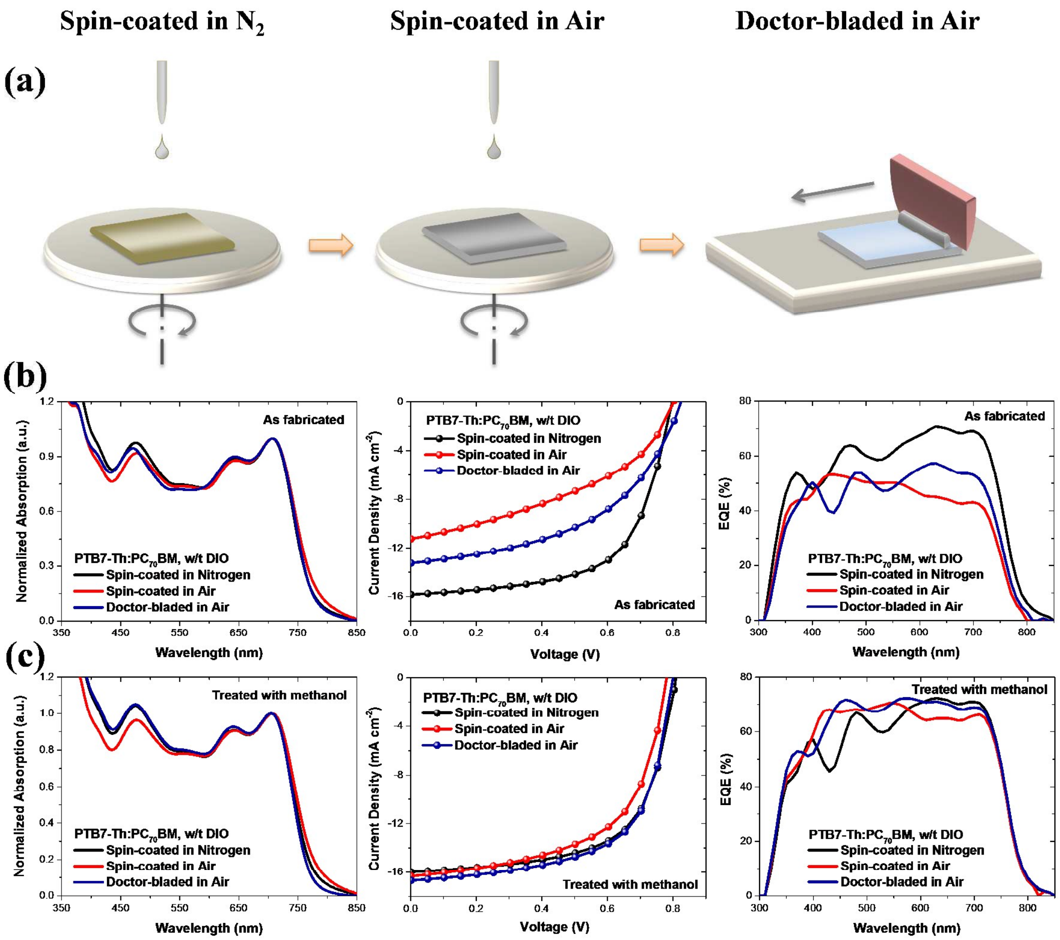

Figure 1 **Materials deposition systems and device characterization.** (**a**) Schematic illustration of the film deposition methods commonly used for the lab-scale OPV devices. Absorption spectra, J-V characteristics and EQE spectra of PTB7-Th based single cells in regular device architecture without (**b**) and with (**c**) methanol treatment.

Table 1 Photovoltaic parameters of the PTB7-Th:PC$_{70}$BM solar cells with and without methanol treatment.

Device	Treatment	V_{OC} [V]	J_{SC} [mA cm^{-2}]	FF [%]	PCE [%]	R_P [kΩ cm^2]	R_S [Ω cm^2]
Spin-coated in N$_2$	-	0.80	15.84	62.1	7.87	1417.7	2.49
	Methanol	0.80	15.99	63.1	8.07	457.2	1.65
Spin-coated in Air	-	0.80	11.23	41.3	3.71	1692.7	2.71
	Methanol	0.78	16.33	58.1	7.40	637.7	1.43
Doctor-bladed in Air	-	0.82	13.25	48.8	5.30	2601.2	3.35
	Methanol	0.80	16.70	62.2	8.31	941.7	1.23

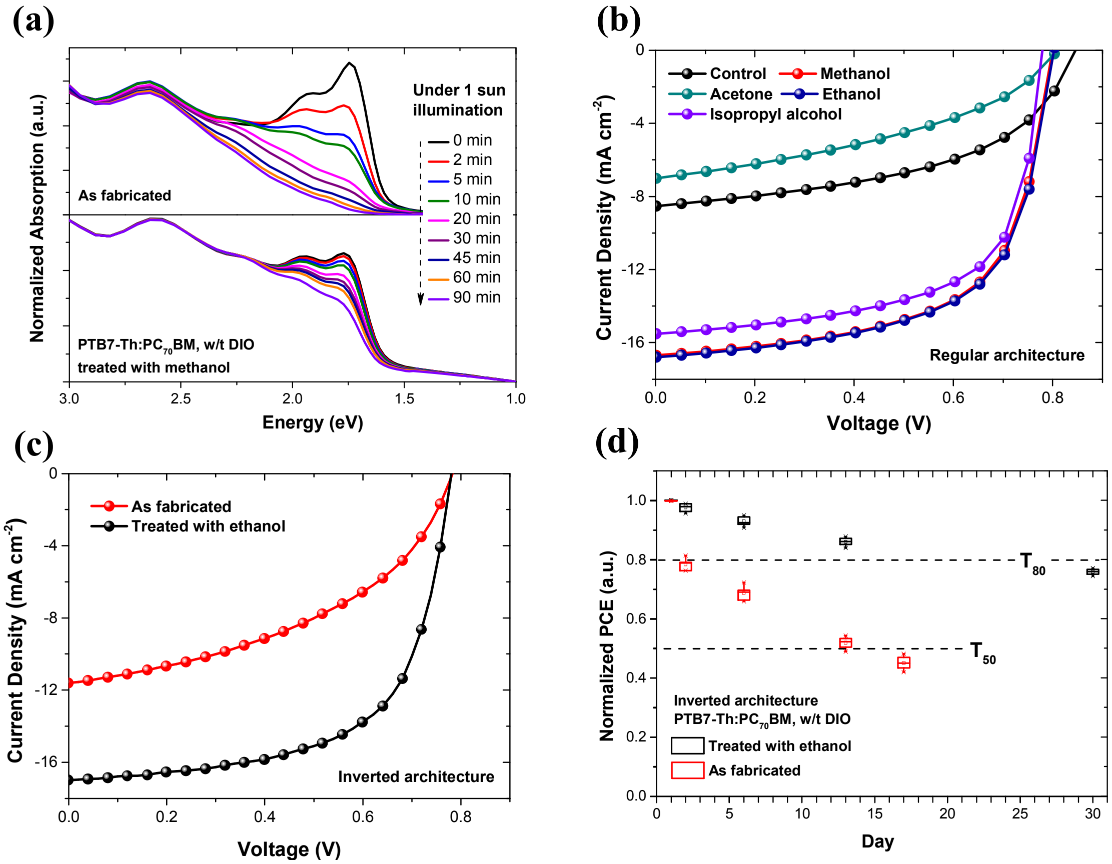

Figure 2 **Device characterization and environmental stability.** (**a**) UV-Vis absorption spectra of PTB7-Th:$PC_{70}BM$ thin films without and with methanol treatment under 1sun illumination for 90 min. The thin films were processed by doctor-blading PTB7-Th:$PC_{70}BM$ with 3% DIO on glass substrates. (**b**) J-V characteristics of PTB7-Th:$PC_{70}BM$ solar cells in a regular architecture treated with various solvents. J-V characteristics (**c**) and environmental stabilities (**d**) of PTB7-Th:$PC_{70}BM$ solar cells in an inverted architecture with and without ethanol treatment. The samples for stability test were kept in air under dark conditions without encapsulation.

Table 2 Photovoltaic parameters of the PTB7-Th:$PC_{70}BM$ solar cells treated with various solvents.

Device	**Architecture**	**V_{OC} [V]**	**J_{SC} [mA cm^{-2}]**	**FF [%]**	**PCE [%]**	**R_P [kΩ cm^2]**	**R_S [Ω cm^2]**
Control	Regular	0.85	8.53	49.8	3.61	2616.2	3.66
Methanol	Regular	0.80	16.70	62.2	8.31	941.7	1.23
Acetone	Regular	0.80	7.01	40.3	2.26	760.2	3.22
Ethanol	Regular	0.80	16.80	62.1	8.35	471.9	1.26
Isopropyl alcohol	Regular	0.78	15.54	64.1	7.77	665.7	1.20
Control	Inverted	0.78	11.61	44.5	4.03	209.5	1.81
Ethanol	Inverted	0.78	16.99	62.6	8.30	174.42	1.37

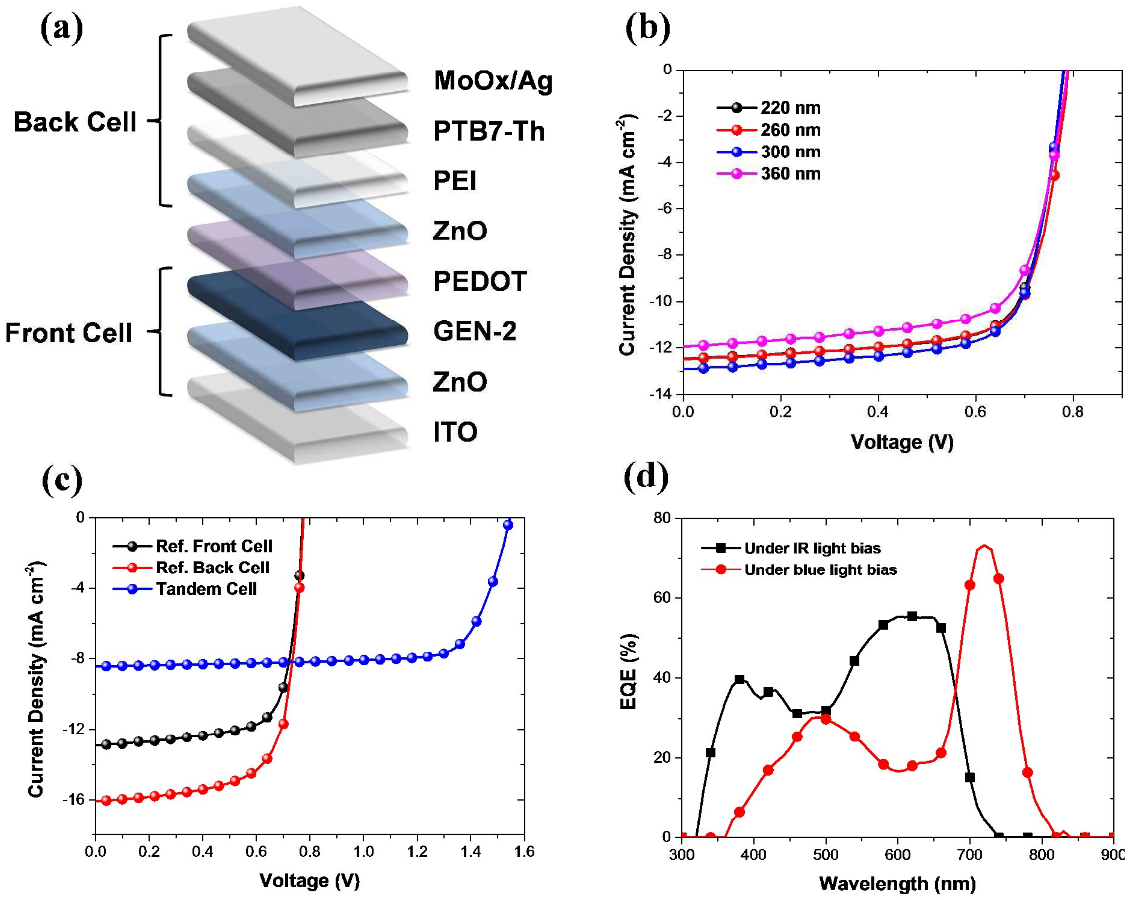

Figure 3 **Device architecture and characterization.** (**a**) Illustration of the inverted device architecture of tandem solar cells fabricated by doctor-blading under ambient conditions and the corresponding sub-cells. (**b**) J-V characteristics of GEN-2:PCBM single cells with different active layer thickness. (**c**) J-V characteristics of the doctor-bladed tandem as well as reference single cells. (**d**) EQE spectra of a tandem solar cell under IR and blue light bias.

Table 3 Photovoltaic parameters of the tandem solar cells based GEN-2:PCBM and PTB7-Th:PC$_{70}$BM and corresponding reference single cells.

Device	Thickness [nm]	V_{OC} [V]	J_{SC} [mA cm^{-2}]	FF [%]	PCE [%]	PCE$_{Best}$ [%]
GEN-2:PCBM	220	0.78	12.47	73.1	7.11	7.18
GEN-2:PCBM	260	0.79	12.51	72.6	7.17	7.28
GEN-2:PCBM	300	0.78	12.92	72.2	7.27	7.31
GEN-2:PCBM	360	0.78	11.96	70.2	6.55	6.99
PTB7-Th:PC$_{70}$BM	120	0.78	16.07	70.0	8.77	9.01
Tandem Cell	300/120	1.55	8.45	76.6	10.03	10.29

Broader Context

All the attraction and advantage of the organic photovoltaics (OPV) technology as compared to other material systems comes from the fact of easy processing by printing or coating under environmental conditions. This is the premise for this technology. Although the power conversion efficiencies (PCEs) of the state-of-the-art OPV devices are steadily improved in the range of 10-12%, the impressive record efficiencies are mainly achieved for devices spin-coated in an inert atmosphere, which does not directly contribute to the commercialization of OPV technology. Compared to the record efficiencies reported for lab processed OPV devices with various architectures, the performance of large-scale produced devices is still at very low levels, which can be mainly attributed to the air-sensitive donor materials as well as the non-optimized large-scale deposition techniques. The benzodithiophene (BDT)-based building blocks have been successfully developed in recent years for constructing high performance polymer donors. Owing to their great photovoltaic properties along with easy processibility, the BDT-polymers are very promising candidates for large-scale production. However, the high-performance BDT- polymers are normally air-instable, and degrade very quickly in the presence of oxygen and light. Thus, the air-instability of the BDT- polymers limits the performance of the air-processed devices, and hinders their applications for large-scale production. Here, we demonstrate that a simple treatment with alcohol solvents can significantly improve the relatively low performance and poor environmental stability of the air-processed OPV devices based on BDT- polymers. Organic tandem solar cells based on a BDT-polymer fabricated by doctor-blading in air achieve high PCE of >10% and FF of >76%.